Adaptive Stereotactic-body Radiation Therapy (SBRT) Planning for Lung Cancer

by

Yujiao Qin

Graduate Program in Medical Physics
Duke University

Date:_____
Approved:

_____
Jing Cai, Supervisor

_____
Fang-Fang Yin, Chair

_____
Shiva Das

_____
Robert Reiman

A thesis submitted in partial fulfillment of
the requirements for the degree of Master of Science in the
Graduate Program in Medical Physics
in the Graduate School of
Duke University

2013

ABSTRACT

Adaptive Stereotactic-body Radiation Therapy (SBRT) Planning for Lung Cancer

by

Yujiao Qin

Graduate Program in Medical Physics
Duke University

Date:_____
Approved:

_____
Jing Cai, Supervisor

_____
Fang-Fang Yin, Chair

_____
Shiva Das

_____
Robert Reiman

An abstract of a thesis submitted in partial fulfillment of
the requirements for the degree of Master of Science in the
Graduate Program in Medical Physics
in the Graduate School of
Duke University

2013

Copyright by
Yujiao Qin
2013

Abstract

Purpose: Tumor size reduction has been observed for patients underwent lung stereotactic body radiation therapy (SBRT). Adaptive planning has the potential to reduce normal tissue toxicity and/or escalate dose to target in these patients. In this study, we evaluated the dosimetric effectiveness of adaptive planning in lung SBRT for patients who presented large target volume changes during the treatment.

Methods and Materials: 20 out of 66 consecutive lung SBRT patients who showed largest percentage internal target volume (ITV) change throughout the treatment were included in the study. All patients went through 3D and 4DCT before treatment, and treatment on a Linear Accelerator machine equipped with kV imager, kV CBCT, and MV electronic portal imaging device (EPID). CBCT images were acquired at each fraction for patient positioning purpose. CBCT images for all fractions were used for contour and treatment planning. Adaptive plans were created on the CBCT images using the same planning parameters as the original CT-based plan, with the goal to achieve comparable conformality index (CI). For each patient, two cumulative plans, non-adaptive plan (P_{NON}) and adaptive plan (P_{ADP}), were generated and compared for the following organs-at-risks (OARs): cord, esophagus, chest wall, and the lungs. Correlations were evaluated between changes in dosimetric metrics induced by adaptive planning and potential impacting factors, including tumor-to-OAR distances ($d_{T\text{-}OAR}$), initial ITV (ITV_1), ITV change (ΔITV), and effective ITV diameter change (Δd_{ITV}).

Results: For the 20 selected patients, percentage ITV change ranged from 16.4% to 59.6%, with a mean (±SD) of 38.8% (±12.5%). CI of all plans ranged from 1.03 to 1.46, with small intra-subject variations (0.01-0.1). Compared to P_{NON}, P_{ADP} resulted in significantly (p=0-0.02) lower values for all dosimetric metrics. $\Delta d_{ITV}/d_{T\text{-}OAR}$ was found to correlate with changes in dose to 5cc (ΔD5cc) of esophagus (r=0.77) and dose to 30cc (ΔD30cc) of chest

wall (r=0.72). Stronger correlations between $\Delta d_{ITV}/d_{T\text{-}OAR}$ and ΔD30cc of chest wall were discovered for peripheral (r=0.82) and central (r=0.94) tumors, respectively.

Conclusions: Adaptive lung SBRT planning can potentially reduce dose to adjacent OARs if patients present significant tumor volume shrinkage during the treatment. Dosimetric benefits of adaptive lung SBRT planning depend upon target volume changes and tumor-to-OAR distances.

Contents

Abstract iv

List of Tables viii

List of Figures ix

Acknowledgements xi

1. Introduction 1

    1.1 Overview of Stereotactic-body Radiation Therapy 1

    1.2 Challenges for Current SBRT Technique 2

    1.3 Adaptive Radiation Therapy 3

    1.4 Aims of this work 3

2. Materials and Methods 5

    2.1 Patient Selection 5

    2.2 Treatment Planning 8

    2.3 Dosimetric Comparison 11

    2.4 Correlation Study 13

3. Results 14

    3.1 Patient Selection 14

    3.2 Dosimetric Comparison for a Representative Patient 18

    3.3 Dosimetric Comparison and Correlation Study for All Selected Patients 21

4. Discussion 28

    4.1 Interpretation of Results 28

4.2 Concerns and Limitations 33

5. Conclusions 37

Appendix – List of Abbreviations 38

References 40

List of Tables

Table 1: Patient characteristics and planning parameters 16

Table 2: Example of adaptive lung SBRT planning for the same patient in Figs. 5-7: comparison of dosimetric metrics between P_{ADP} and P_{NON} 20

Table 3: Comparision of dosimetric metrics between non-adaptive treatment planning (P_{NON}) and adaptive treatment planning (P_{ADP}) for the 20 selected patients..... 22

List of Figures

Figure 1: Example of a representative patient's CBCT image with the window/level of -80/2000 6

Figure 2: Illustration of the typical beam arrangement for the original CT plan..... 8

Figure 3: Trans-axial contour of the chest wall (in yellow) for the same patient in Fig.1, on CBCT images of all 4 fractions. 9

Figure 4: Flow chart illustration of deformable registration and dose summation for adaptive planning: (a) before registration, CBCT images and their associated doses; (b) after registration, deformed $CBCT_2$-$CBCT_N$ images and their associated deformed doses based on $CBCT_1$. 11

Figure 5: Changes of percentage ITV throughout the course of treatment for 40 lung SBRT patients. Colored lines indicate the 20 patients with the largest percentage ITV changes. 14

Figure 6: Example of adaptive lung SBRT planning for a representative patient: isodose lines of adaptive plans on fractional CBCT images. 18

Figure 7: Example of adaptive lung SBRT planning for the same patient in Fig. 5: comparison of DVHs between the adaptive plan (P_{ADP}, solid lines) and the non-adaptive plan (P_{NON}, dotted lines). 19

Figure 8: Example of adaptive lung SBRT planning for the same patient in Figs. 5-6: plot of comparison of dosimetric metrics between P_{ADP} and P_{NON} 20

Figure 9: Correlation between $\Delta d_{ITV}/d_{T\text{-}OAR}$ and ΔD5cc of esophagus. 23

Figure 10: Correlation between $\Delta d_{ITV}/d_{T\text{-}OAR}$ and ΔD30cc of chest wall. 23

Figure 11: Correlation between $\Delta d_{ITV}/d_{T\text{-}OAR}$ and ΔD30cc of chest wall for peripheral tumors 25

Figure 12: Correlation between $\Delta d_{ITV}/d_{T\text{-}OAR}$ and ΔD30cc of chest wall for central tumors 25

Figure 13: Correlation between $\Delta d_{ITV}/d_{T\text{-}OAR}$ and ΔD0.35cc of cord with (r=0.24) and without (r=0.71) the two IMRT cases with tight cord constraints (red points) 26

Figure 14: Correlation between $\Delta d_{ITV}/d_{T\text{-}OAR}$ and ΔD1.2cc of cord with (r=0.29) and without (r=0.75) the two IMRT cases with tight cord constraints (red points) 27

Figure 15: CT plan of one of the two IMRT cases with tight cord constrains. Orange contour represents the cord; thick yellow isodose line is 100%; outermost green isodose line is 30%..... 27

Figure 16: Correlation between $\Delta d_{ITV}/d_{T\text{-}OAR}$ and ΔD5cc of esophagus for 20 selected patients (blue points, blue trend line, blue r value), and 26 patients (all points, red trend line, red r value) with 6 additional small-ITV-change patients in red. 30

Figure 17: Correlation between $\Delta d_{ITV}/d_{T\text{-}OAR}$ and ΔD30cc of chest wall for 20 selected patients (blue points, blue trend line, blue r value), and 26 patients (all points, red trend line, red r value) with 6 additional small-ITV-change patients in red. 31

Figure 18: Correlation between $\Delta d_{ITV}/d_{T\text{-}OAR}$ and ΔD0.35cc of spinal cord for 20 selected patients (blue points, blue trend line, blue r value), and 26 patients (all points, red trend line, red r value) with 6 additional small-ITV-change patients in red. 31

Figure 19: Correlation between $\Delta d_{ITV}/d_{T\text{-}OAR}$ and ΔD1.2cc of spinal cord for 20 selected patients (blue points, blue trend line, blue r value), and 26 patients (all points, red trend line, red r value) with 6 additional small-ITV-change patients in red. 32

Figure 20: Overlay of CBCT4 and CBCT1 (same case as illustrated in Figs. 5-7 and Table 3) (a) after rigid registration but before deformable image registration; and (b) after both the rigid and deformable image registration. Red arrows indicate good matches for trachea and soft tissues, while yellow arrows indicate largely maintained differences in tumor volumes (greyscale areas). 35

Acknowledgements

I would like to express my deep gratitude to Dr. Jing Cai, my research advisor for his patient guidance, constructive critiques, and enthusiastic encouragement of this research work. I would also like to thank Dr. Fang-Fang Yin, my research supervisor in his constructive recommendations throughout the study. My grateful thanks are also extended to Dr. Chris Kelsey and Dr. David Yoo for their great help and suggestions in patient selection and tumor contouring. I would also like to thank Ms. Fan Zhang for her help in contouring organs-at-risk at the early stage of this study.

1. Introduction

1.1 Overview of Stereotactic-body Radiation Therapy

Patients with early stage, medically inoperable lung cancer have a poor local control rate (30%-40%) and a high mortality rate (3-year survival, 20%-35%) with conventional radiation therapy [1, 2]. The ineffectiveness of conventional radiation therapy is partially related to the complex geometrical and biological uncertainties that exist throughout the course of treatment, such as respiratory motion, intra/inter-fractional variations, and changes in response to treatment. Reduction of these uncertainties can potentially reduce radiation exposure to organs-at-risk (OARs), allow for dose escalation, and subsequently improve local control and survival.

Compared to conventional radiation therapy, stereotactic-body radiotherapy (SBRT) delivers much higher dose to the target in much fewer fractions (3 to 5). Sharper dose fall-off at the edge of target requires SBRT to have accurate target volume delineation mechanisms. Advanced imaging techniques like 4DCT, kilovoltage (kV) planar imaging, and kV cone-beam CT (CBCT) were commonly used to reduce uncertainties in tumor volume delineation and patient positioning. These improvements help reduce radiation toxicity to OARs and allow for dose escalation to the target for SBRT. As opposed to conventional radiation therapy, it has been shown that SBRT is

effective for treating early-stage non-small cell lung cancers (NSCLC) or oligometastatic lesions in the lung [3, 4].

1.2 Challenges for Current SBRT Technique

Despite improved local control and survival rate, SBRT for lung cancer still faces challenges in terms of the reduction of radiation toxicity of normal tissues and dose escalation to the target. For example, multiple trials report 20% to 30% incidence rate of chest wall toxicity in patients who received more than 30 Gy in lung SBRT [5,6]. Esophagitis and skin reactions are relatively rare, but have been observed when the tumor is close to the esophagus or skin [7]. Moreover, Takeda *et al* reported that the 2-year control rate for oligometastatic lung tumors from colorectal cancer (72%) is significantly worse than that from other origins or from primary lung cancer (94%-95%) after SBRT [8]. Further dose escalation may be desired for metastatic lesions in the lung from certain primary sites in order to achieve good local control. However, the question remains whether it is possible to reach a radiation dose level of 100 Gy BED or higher in centrally located tumors without causing excessive toxicity to the normal tissues. For instance, Timmerman *et al.* suggested that SBRT to a dose of between 60 Gy and 66 Gy delivered in 3 fractions, was inappropriate for centrally located primary lung tumors because the 2-year freedom from sever toxicity rate was 54% [6]. Tackling these challenges demands

further reduction of margins associated with PTV in lung SBRT. Margin reduction may be possible since tumor volume and tumor motion may change in response to treatment.

1.3 Adaptive Radiation Therapy

Adaptive radiation therapy (ART) utilizes an active feedback loop to modify plans based on updated information during the course of treatment. The adaptation is usually defined for the changes in tumor size, shape, and position observed in images acquired at different times throughout the treatment [17]. ART therefore has the potential to further reduce margin associated with PTV, especially for patients with larger tumor motion or inter-fractional tumor volume reduction.

For patients treated with SBRT, significant tumor size reduction throughout the treatment has been reported [17]. Since the target volume is usually small and a large fraction of radiation dose is delivered in less than 5 fractions, missing a small volume of target in even just one fraction can cause significant underdosing of the tumor and/or overdosing of the surrounding normal tissues. Adaptive lung SBRT is therefore highly desired, for it has the potential to mitigate radiation exposure to OARs and/or further escalate dose to the tumor for these patients.

1.4 Aims of this work

The first aim of this study was to assess the effectiveness of adaptive lung SBRT planning in terms of dosimetric advantages to the normal tissues and/or target. In order

to do that, patients who presented large target volume changes during SBRT treatment were selected as candidates. Adaptive plans were retrospectively carried out for these patients. Dosimetric analysis was performed to determine if adaptive SBRT significantly reduced dose to normal tissues.

The second aim of our study was to identify patient-specific factors that led to significant OAR dose sparing, so that we know which patient would benefit more from the adaptive strategy. This was done via correlation studies of dose sparing at various OARs, versus several proposed patient-specific factors. Strong correlations discovered were further analyzed for their robustness and repeatability.

2. Materials and Methods

2.1 Patient Selection

This study aimed to quantitatively evaluate potential dosimetric benefits of adaptive planning for lung SBRT patients who presented relatively larger target volume changes during the treatment. Patients with small target volume changes are less likely to profit from adaptive planning due to anticipated small dosimetric changes, and therefore were not the interest of this study.

To identify patients who are suitable for this retrospective adaptive planning study, 66 consecutive patients (31 female, 35 male, mean age of 73.0) who had lung SBRT treatment at our institution were initially included. Lung SBRT treatments were delivered on a Linear Accelerator machine equipped with kV imager, kV CBCT, and MV electronic portal imaging device (EPID). CBCT was acquired before each fraction for patient positioning verification purposes.

Two radiation oncologists with expertise in lung SBRT contoured the visible tumors on the CBCT images of all fractions for the 66 patients. A consistent window/level of -80/2000 was used for target contouring. As shown in Fig. 1, lung tissues were clearly visible at this window/level for CBCT, while the tumor remained distinguishable from the surrounding tissue for target volume delineation.

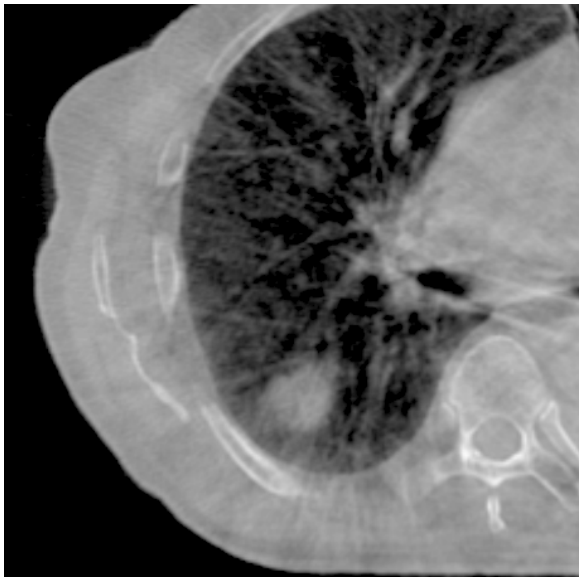

Figure 1: Example of a representative patient's CBCT image with the window/level of -80/2000

Since the tumor volume on CBCT is a mix of tumor volume and tumor motion, the contoured volume was the internal target volume (ITV) [9]. Consistency of CT number was checked between fractional CBCT images for each patient. Inter-modality (CBCT versus CT) and inter-observer variance in target volume contouring has been investigated in the literature, and minimal differences were found [10]. Out of the 66 patients, 26 patients with small tumors (first fraction ITV < 1 cm^3), tumors adjacent to soft tissues, and poor CBCT image quality, were firstly excluded from the study to avoid uncertainties in target volume delineation. The remaining 40 patients were further analyzed based on their inter-fractional ITV change.

Relative ITV change was used as the metric for patient selection for adaptive lung SBRT planning. For each of the 40 patients, the overall relative ITV change

throughout the treatment was determined as the ratio of the ITV of the last fraction (ITV_N) to the ITV of the first fraction (ITV_1). All patients were ranked according to their overall relative ITV change. Adaptive planning was carried out starting from those with the larger overall relative ITV changes. Methods for adaptive planning were discussed in detail in the following subsection of this chapter. After adaptive planning, it was observed that in our study, patients with less than 15% relative ITV change presented minimal difference between the adaptive plan and the original plan. Minimal dosimetric difference was anticipated for these patients, and they were further excluded from the study.

The remaining 20 patients with larger relative ITV changes (>15%) were therefore selected for the adaptive planning study. Table 1 summarizes the characteristics of the selected 20 patients. Adaptive planning was carried out; dosimetric comparison and correlation studies were performed subsequently for these patients.

2.2 Treatment Planning

For all selected patients, the original CT plans were created on the 3DCT images using Eclipse (Varian Medical Systems). 8 to 14 coplanar beams were arranged in a fan shape around the target. Fig. 2 illustrates the beam arrangement on the original CT plan of one representative patient. Gross tumor volumes (GTVs) were contoured on the maximum intensity projection (MIP) image of the 4DCT by the physicians, and the OARs were contoured on the average intensity projection (AIP) image by the dosimetrists. Planning target volumes (PTVs) were generated by adding a 5mm uniform margin around the GTV.

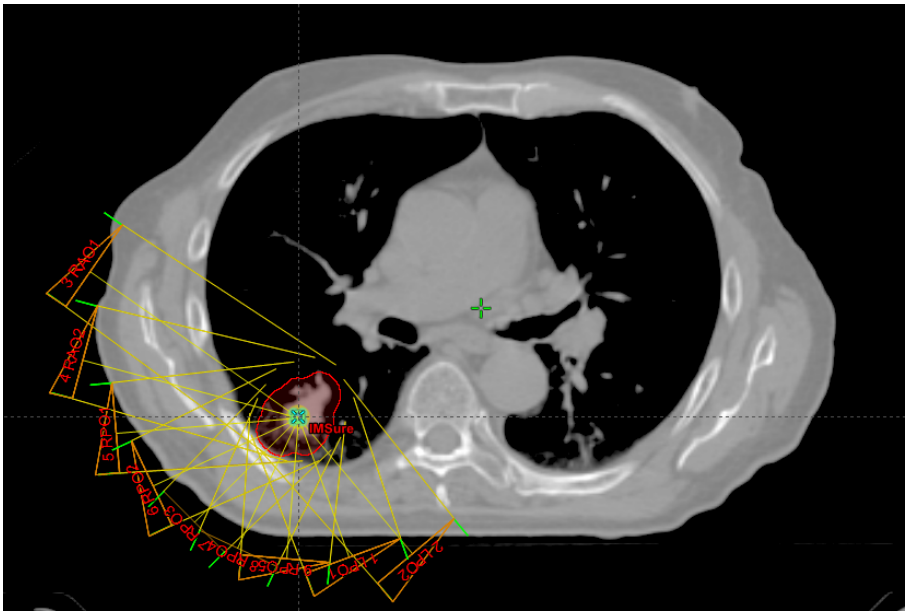

Figure 2: Illustration of the typical beam arrangement for the original CT plan

For our study, all plans were created on CBCT images using Eclipse. PTVs were generated by adding a same 5 mm uniform margin on the ITVs. OARs included the

lungs, spinal cord, esophagus, and chest wall. As shown in Fig. 3, chest wall was contoured as the 3 cm thick region around the exterior wall of lung, extended 4 slices further than the superior and inferior ends of the PTV (in superior and inferior directions, respectively). All OAR contours were approved by experienced clinical physicist.

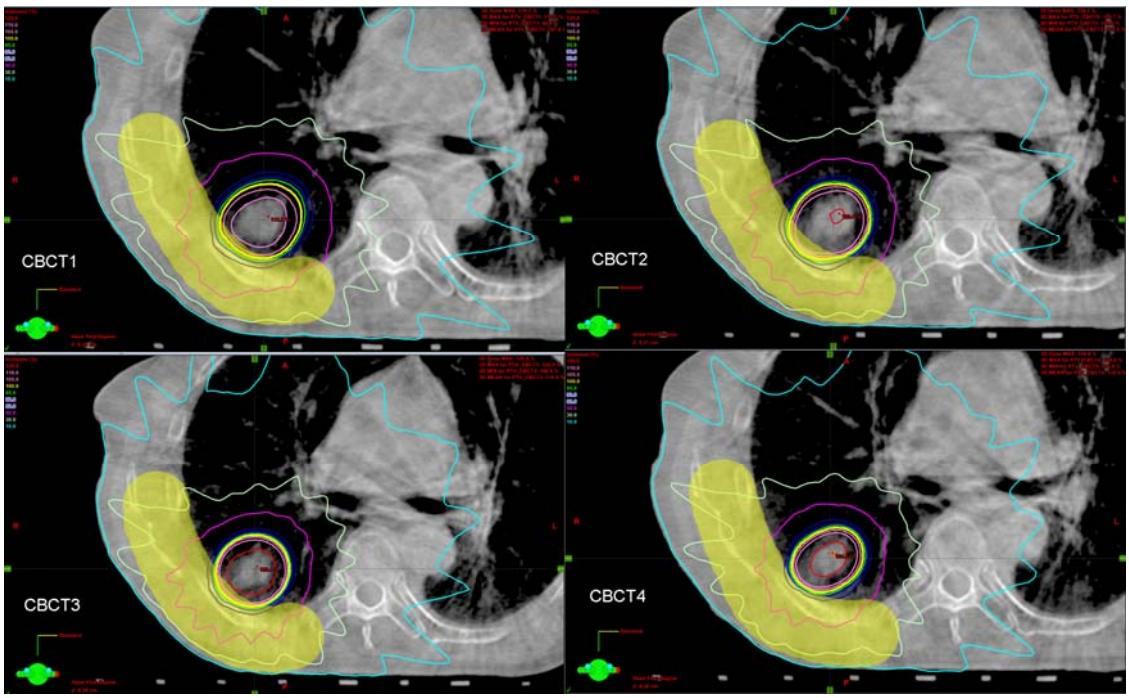

Figure 3: Trans-axial contour of the chest wall (in yellow) for the same patient in Fig.1, on CBCT images of all 4 fractions.

For adaptive planning, P_{ADP}, original plans generated on the planning CT were first copied onto CBCT images, followed by alignment of beams to the centers of the new PTVs. Beam parameters were kept the same as the original plan except for MLC leaf

positions, which were adjusted to fit the new PTVs. The objective of adaptive planning was to achieve comparable conformality index (CI) to that of the original CT plan.

Out of the 20 selected patients, 15 patients had 3D-CRT plans and 5 patients had IMRT plans. For the 3D-CRT plans, MLC leaf positions of each beam were manually adjusted based on the new PTV. This process was repeated until the satisfied CI was achieved. For the IMRT plans, re-optimization was performed using the same normal tissue and PTV constrains and priorities. All plans were normalized so that 95% of the PTV was covered by 100% of the prescription dose.

Accumulated dose of P_{ADP} was determined using deformable image registration implemented in commercial software (Velocity AI, Velocity Medical System, Atlanta, GA). For each patient, CBCT image of the first fraction ($CBCT_1$) were used as the reference; CBCT images of other fractions ($CBCT_2$ to $CBCT_N$) were first rigidly registered to $CBCT_1$, and then non-rigidly using a multi-pass deformable registration. Registration results were visually inspected based on landmarks of patient anatomy. The primary goal of registration was to achieve good match in the OARs. Repeated registrations were performed in cases where first registration failed to achieve the goal. Doses associated with $CBCT_2$ to $CBCT_N$ were also deformed according to the respective image deformations. The deformed doses of the later fractions were then summed up with the first fraction dose to generate the accumulative adaptive dose of P_{ADP}.

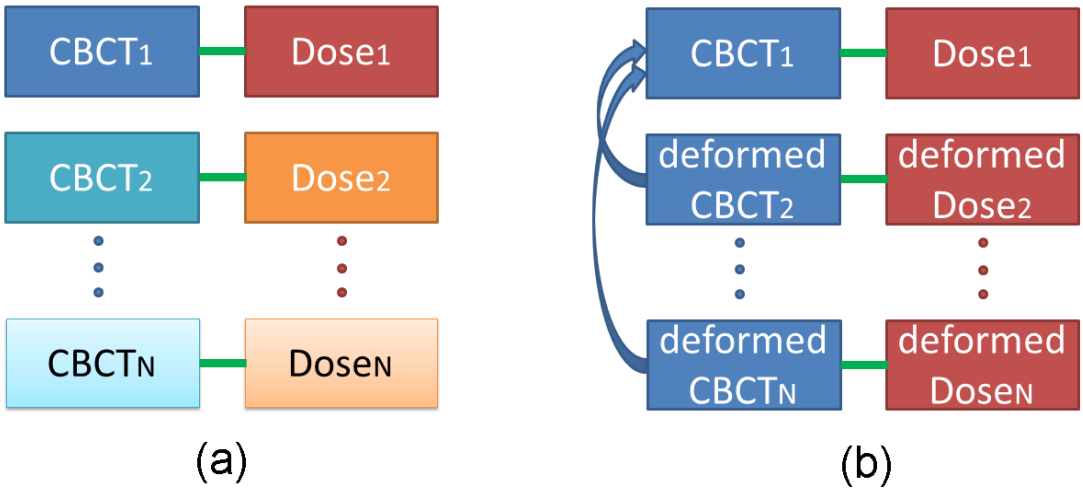

Figure 4: Flow chart illustration of deformable registration and dose summation for adaptive planning: (a) before registration, CBCT images and their associated doses; (b) after registration, deformed $CBCT_2$-$CBCT_N$ images and their associated deformed doses based on $CBCT_1$.

For non-adaptive planning P_{NON}, accumulated dose was determined simply by multiplying dose of the first fraction (same as the dose of the first fraction of P_{ADP}) by the number of fractions. It should be noted that both P_{ADP} and P_{NON} were based on CBCT plans. The same imaging modality was used for all dosimetric comparisons in the next subsection.

2.3 Dosimetric Comparison

Dose files of P_{NON} and P_{ADP} were exported from Velocity AI for further analysis. Dose volume histograms (DVHs) were compared between P_{NON} and P_{ADP} for the following dosimetric metrics: D1000cc and D1500cc of lungs, D0.35cc and D1.2cc of cord, maximum dose (Dmax) to the cord, D5cc of esophagus, maximum dose to the esophagus. These metrics were selected based on the recommendation of Radiation

Therapy Oncology Group (RTOG) 0915. Two additional metrics, V20Gy of lungs and D30cc to chest wall, were also included. V20Gy is a commonly used clinical DVH parameter; D30cc of chest wall was selected based on a recent study suggesting that cumulative doses over 30Gy at 30cc of chest wall can cause severe chest pain and rib fracture [11, 12].

Due to the limited field of view (FOV) of CBCT, some OARs, such as the lungs, were only partially imaged in CBCT. Percentage volume parameters based on CT lung volumes would not be precise for these OARs. To be consistent, all metrics were recorded in absolute values of Gy and cc. Absolute differences between P_{NON} and P_{ADP} for these OAR metrics were calculated.

Two metrics for the target volumes were also included: D95% of PTV and D100% of ITV. It should be noted that the PTV/ITV here refer to the first fraction PTV/ITV. Since target volume changed by a large extent from fraction to fraction for the selected patients, the dose differences between P_{NON} and P_{ADP} for these two metrics were expected to be large. Significant dose reduction on PTV_1/ITV_1 here does not mean target under-dosing.

For each metric, the mean and standard deviation (SD) of P_{NON} and P_{ADP} for all 20 patients were recorded. The statistical significance of the comparison was also evaluated using a paired t-test at a significance level of 0.05. Table 3 compiles the p values for all the metrics.

2.4 Correlation Study

It is of clinical interest to be able to identify candidates who would benefit from the adaptive SBRT strategy prior to treatment. Possible predicting factors associated with intrinsic patient characteristics would help identify potential candidates. In order to discover these predicting factors, correlation studies were carried out between dosimetric differences from adaptive planning (ΔD) in various OAR metrics and several patient-specific factors. These factors include tumor-to-OAR distances ($d_{T\text{-}OAR}$), initial ITV (ITV_1), absolute change of ITV ($\Delta ITV = ITV_N - ITV_1$), and change of effective ITV diameter ($\Delta d_{ITV} = d_{ITV_N} - d_{ITV_1}$, where $d_{ITV} = (3*ITV/4\pi)^{(1/3)}*2$). $d_{T\text{-}OAR}$ was measured as the distance from the center of ITV to the center of the OAR.

The following OAR dosimetric metrics were studied: D0.35cc and D1.2cc of cord, D5cc of esophagus, and D30cc of chest wall. All lung metrics (D1000cc, D1500cc and V20Gy) were excluded from the correlation study because the ΔD for lung metrics were observed to be minimal after adaptive planning. Dmax of cord and Dmax of esophagus were also excluded because maximum dose can be very sensitive to single pixel value, any trend observed in ΔD versus potential impacting factors may not be accurate representation.

3. Results

3.1 Patient Selection

Figure 5 compiles the relative ITV changes for the 40 patients. 20 patients (9 male, 11 female, mean age 73.1) indicated by colored lines were selected for the adaptive planning study. Grey lines represent the 20 patients with smaller relative ITV change (<15%), which lead to minimal difference in their adaptive plans, and subsequently minimal dose sparing expected for the OARs.

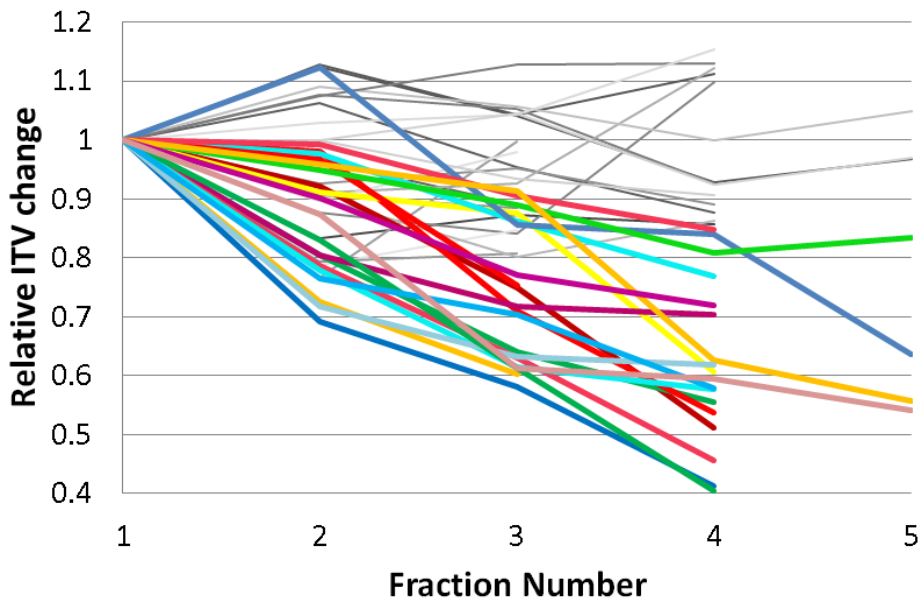

Figure 5: Changes of percentage ITV throughout the course of treatment for 40 lung SBRT patients. Colored lines indicate the 20 patients with the largest percentage ITV changes.

Table 1 compiles the characteristics of the 20 selected patients: ITV_1 ranged from 1.92 cm^3 to 135.13 cm^3; Percentage ITV change ranged from 16.4% to 59.6%, with a mean (±SD) of 38.8% (±12.5%); Mean (±SD) distance from tumor to cord, esophagus, and chest

wall was 8.32 (±3.64) cm, 7.37 (±2.08) cm, and 3.68 (±1.29) cm, respectively; Of all treatment plans, CI ranged from 1.03 to 1.46, with small intra-subject variations (SD of CI ranged from 0.01 to 0.10).

Table 1: Patient characteristics and planning parameters

Patient	Age	Gender	Prescription	Planning Technique	Tumor location	ITV		% ITV Change	CI mean(±SD)	Tumor to Cord Distance (cm)	Tumor to Esophagus Distance (cm)	Tumor to Chest Wall Distance (cm)
						ITV_1 (cm^3)	ITV_N (cm^3)					
1	57	F	12Gy x 4	3D-CRT	C,ULL	1.92	1.11	42.2%	1.29 (±0.10)	3.01	4.31	2.26
2	86	M	18Gy x 3	3D-CRT	C,CRL	2.15	1.62	24.7%	1.22 (±0.06)	10.56	8.43	5.32
3	64	M	12.5Gy x 4	3D-CRT	P,ULL	3.31	2.38	28.1%	1.32 (±0.04)	16.52	11.01	2.85
4	66	F	10 Gy x 5	3D-CRT	C,CLL	3.33	1.8	46.0%	1.39 (±0.04)	5.01	3.75	5.18
5	72	M	9 Gy x 5	3D-CRT	C,CRL	3.55	1.98	44.2%	1.33 (±0.07)	6.52	7.07	5.37
6	42	M	18 Gy x 3	3D-CRT	P,CRL	3.72	2.24	39.8%	1.37 (±0.04)	9.09	8.13	2.33
7	84	F	12 Gy x 4	3D-CRT	P,CRL	4.03	1.66	58.8%	1.15 (±0.05)	10.35	9.18	2.33
8	71	F	12 Gy x 4	3D-CRT	P,CLL	5.31	3.73	29.8%	1.29 (±0.03)	13.64	9.98	2.71
9	67	M	10 Gy x 5	IMRT	P,URL	8.73	5.55	36.4%	1.27 (±0.03)	9.2	6.08	2.96
10	85	M	12.5 Gy x 4	3D-CRT	P,RCL	8.96	3.62	59.6%	1.12 (±0.05)	6.77	8.81	3.54
11	77	F	12 Gy x 4	3D-CRT	C,ULL	8.97	6.89	23.2%	1.19 (±0.03)	4.16	4.91	3.8
12	81	M	12 Gy x 4	3D-CRT	P,CRL	9.51	5.49	42.3%	1.46 (±0.07)	14.77	-	2.92
13	58	F	12 Gy x 4	3D-CRT	P,LLL	13.95	8.46	39.4%	1.41 (±0.05)	7.22	10.02	2.07
14	77	F	12 Gy x 4	3D-CRT	C,CLL	14.02	6.38	54.5%	1.20 (±0.07)	6.67	5.4	-
15	80	F	10 Gy x 5	3D-CRT	C,CLL	17.37	14.48	16.6%	1.22 (±0.08)	8.42	6.2	5.24
16	72	M	12 Gy x 4	3D-CRT	P,CRL	24.5	13.15	46.3%	1.16 (±0.02)	10.19	9.7	3.76
17	86	F	12 Gy x 4	IMRT	C,URL	25.38	15.67	38.3%	1.42 (±0.04)	3.49	7.11	2.58

18	58	F	12 Gy x 4	IMRT	P,ULL	35.33	29.54	16.4%	1.17 (±0.02)	6.29	6.35	4.27
19	95	F	12 Gy x 4	IMRT	C,ULL	111.25	65.81	40.8%	1.03 (±0.01)	5.69	6.05	4.17
20	84	M	12 Gy x 4	IMRT	C,CRL	135.13	69.08	48.9%	1.06 (±0.03)	8.9	7.48	6.31
Mean (±SD)	73.1 (±13.0)	-	-	-	-	22.02 (±35.95)	13.03 (±19.84)	38.8% (±12.5%)	1.25 (±0.05)	8.32 (±3.64)	7.37 (±2.08)	3.68 (±1.29)

3.2 Dosimetric Comparison for a Representative Patient

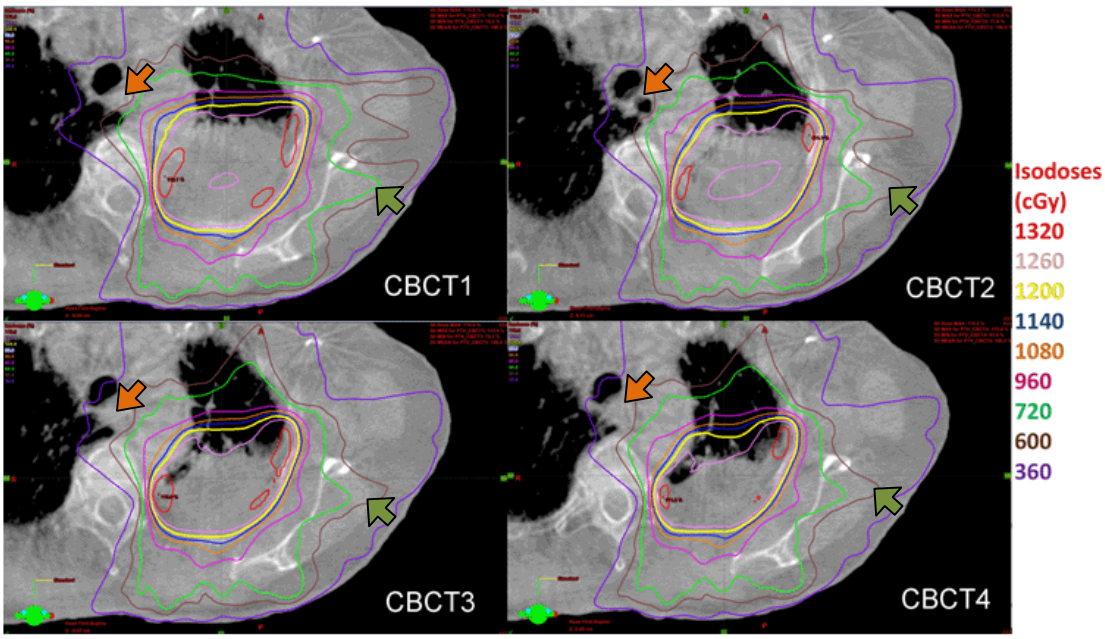

Figure 6: Example of adaptive lung SBRT planning for a representative patient: isodose lines of adaptive plans on fractional CBCT images.

Figure 6 shows adaptive lung SBRT plans for a representative patient. Changes in the isodose lines can be readily seen on the fractional CBCT images. Yellow line represents the 100% isodose. It was greatly reduced from $CBCT_1$ to $CBCT_4$ due to the ITV reduction. Changes in the isodose lines around the esophagus (orange arrows) and chest wall (green arrows) indicate dose sparing for these OARs for this particular patient.

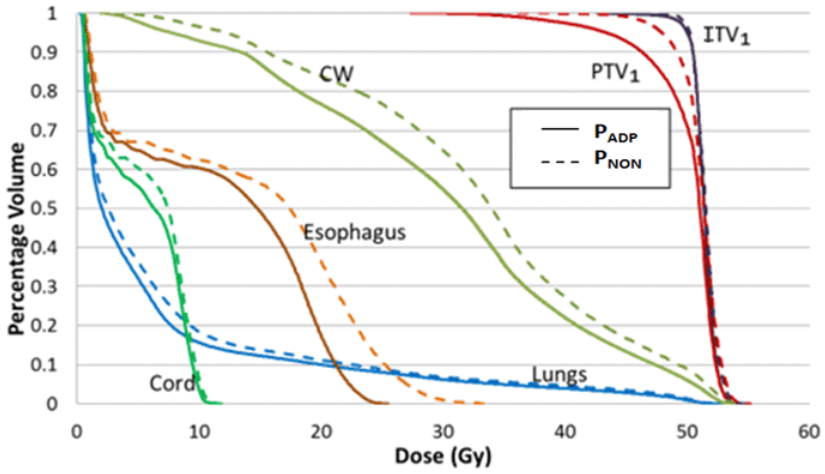

Figure 7: Example of adaptive lung SBRT planning for the same patient in Fig. 5: comparison of DVHs between the adaptive plan (P_{ADP}, solid lines) and the non-adaptive plan (P_{NON}, dotted lines).

The same OAR dose sparing can be observed in the DVH plots of this patient (Fig. 7). For esophagus and chest wall, large separations exist between the DVHs of P_{NON} (dotted lines) and P_{ADP} (solid lines), indicating significant dose sparing after adaptive planning. Large dose differences are also observed in Fig. 8, the dose metric plots, between P_{NON} and P_{ADP} for the esophagus metrics.

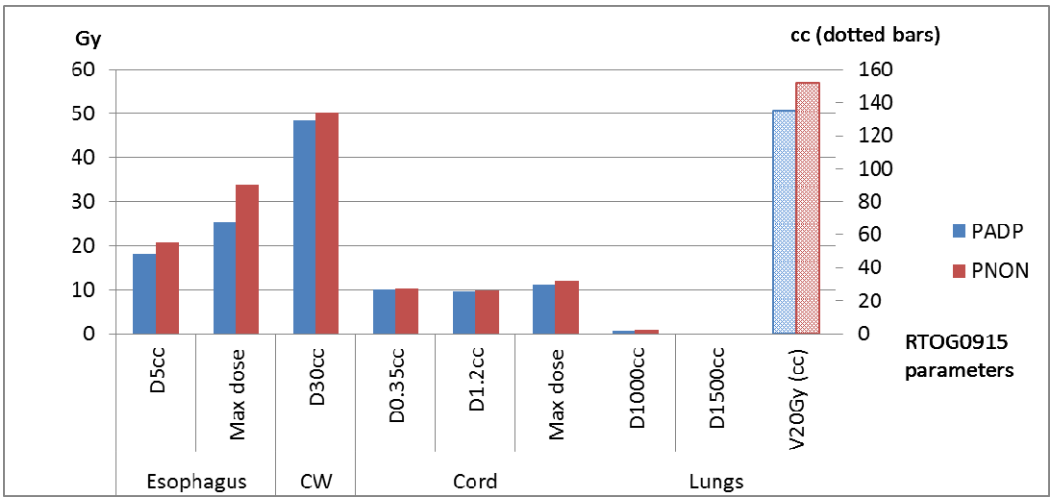

Figure 8: Example of adaptive lung SBRT planning for the same patient in Figs. 5-6: plot of comparison of dosimetric metrics between P_{ADP} and P_{NON}

Table 2: Example of adaptive lung SBRT planning for the same patient in Figs. 5-7: comparison of dosimetric metrics between P_{ADP} and P_{NON}

		P_{ADP}	P_{NON}
Esophagus	D5cc(Gy)	18.27	20.85
	Max dose(Gy)	25.49	33.87
CW	D30cc(Gy)	48.34	50.09
Cord	D0.35cc(Gy)	10.16	10.44
	D1.2cc(Gy)	9.62	9.90
	Max dose(Gy)	11.29	12.03
Lungs	D1000cc	0.86	1.03
	D1500cc	0	0
	V20Gy (cc)	135.32	151.49
PTV_1	D95%(Gy)	43.38	47.93
ITV_1	D100%(Gy)	53.97	55.09

Table 2 lists the numerical values of the metrics plotted in Fig. 7 in both adaptive and non-adaptive plans. For esophagus, Dmax was 33.9 Gy and 25.5 Gy in P_{NON} and P_{ADP}, respectively; D5cc was 20.8 Gy and 18.3 Gy in P_{NON} and P_{ADP}, respectively. Noting that

constraints for Dmax and D5cc of esophagus are 30 Gy and 18.8 Gy respectively in RTOG 0915, these results indicated that P_{ADP} was able to reduce esophagus doses to meet the RTOG criteria. Dose sparing for the OARs as a result of adaptive strategy is always preferred, but such effect is most beneficial to patients when the normal tissue toxicity is reduced to below the RTOG thresholds. In this patient's case, adaptive lung SBRT is able to not only reduce dose to all OARs of interest, but also save the esophagus from the endpoint of stenosis and/or fistula, according to RTOG 0915.

It should be noted that the PTV and ITV shown in Fig. 8 is the PTV and ITV of the first fraction (PTV_1 and ITV_1), which received less dose coverage as a result of adaptive planning. The true PTV and ITV varied at each fraction, and 95% of the true PTV always received 100% of the prescription dose at each fraction.

3.3 Dosimetric Comparison and Correlation Study for All Selected Patients

Table 3 summarizes the results of dosimetric comparisons for all 20 patients. Compared to P_{NON}, P_{ADP} significantly ($p<0.02$) reduced dose for all OAR metrics. Therefore, we can conclude that for selected patients of large tumor volume reductions, adaptive lung SBRT is able to spare dose to adjacent OARs while maintaining target coverage.

Again, the PTV_1 and ITV_1 represent the first fraction PTV and ITV respectively. It should be noted that ITVs contoured on the CBCTs were smaller than ITV of the original CT image, due to the underestimation of ITV for free-breathing CBCT patients with

irregular breathing patterns [19]. This ITV difference does not affect the accuracy of our results, since both plans were generated based on CBCT ITVs.

Table 3: Comparision of dosimetric metrics between non-adaptive treatment planning (P_{NON}) and adaptive treatment planning (P_{ADP}) for the 20 selected patients

		Mean (±SD)		P value
		P_{ADP}	P_{NON}	
Lungs	D1000cc (Gy)	2.58 (±1.60)	2.83 (±1.82)	0.01
	D1500cc (Gy)	1.26 (±1.02)	1.42 (±1.22)	0.02
	V20Gy (cc)	162.45 (±92.16)	176.36 (±101.87)	0.00
Cord	D0.35cc (Gy)	9.75 (±4.37)	10.79 (±4.14)	0.01
	D1.2cc (Gy)	8.77 (±3.95)	9.68 (±3.75)	0.01
	Max Dose (Gy)	11,08 (±5.09)	12.34 (±4.89)	0.01
Esophagus	D5cc (Gy)	8.74 (±4.51)	9.56 (±5.06)	0.00
	Max Dose (Gy)	15.18 (±6.62)	16.53 (±7.70)	0.02
CW	D30cc (Gy)	27.88 (±8.18)	29.33 (±8.73)	0.00
PTV_1	D95% (Gy)	47.46 (±2.86)	49.37 (±2.41)	0.00
ITV_1	D100% (Gy)	50.21 (±3.99)	51.52 (±3.44)	0.02

Fig. 9-14 illustrates the results of the correlation studies. Ratio of effective ITV diameter change and tumor-to-OAR distance ($\Delta d_{ITV}/d_{T\text{-}OAR}$) was found to be linearly correlated with ΔD5cc of esophagus (r=0.77) and ΔD30cc of chest wall (r=0.72) as shown in Fig. 8-9. This means for the selected patients, larger Δd_{ITV} and shorter $d_{T\text{-}OAR}$ contribute to greater dose sparing at the esophagus and chest wall metrics. Separate studies between Δd_{ITV} versus ΔD, and $d_{T\text{-}OAR}$ versus ΔD achieve no such strong correlation for esophagus or chest wall. This may be due to the fact that both factors of Δd_{ITV} and $d_{T\text{-}OAR}$ contribute equally to the dose sparing of adaptive strategy. One thing to notice is that Δd_{ITV} was initially calculated using absolute ITV change (ΔITV). Therefore,

the positive correlation between $\Delta d_{ITV}/d_{T\text{-}OAR}$ and ΔD also means ΔITV contribute positively to ΔD of esophagus and chest wall, although non-linearly.

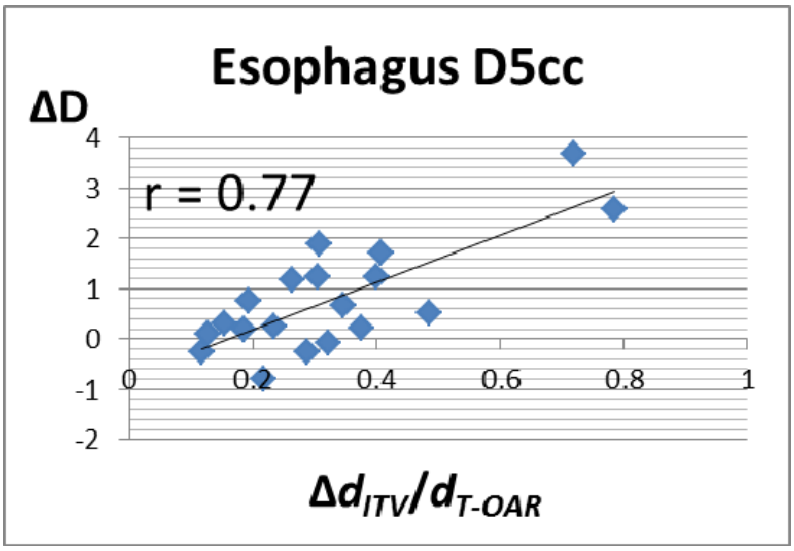

Figure 9: Correlation between $\Delta d_{ITV}/d_{T\text{-}OAR}$ and ΔD5cc of esophagus.

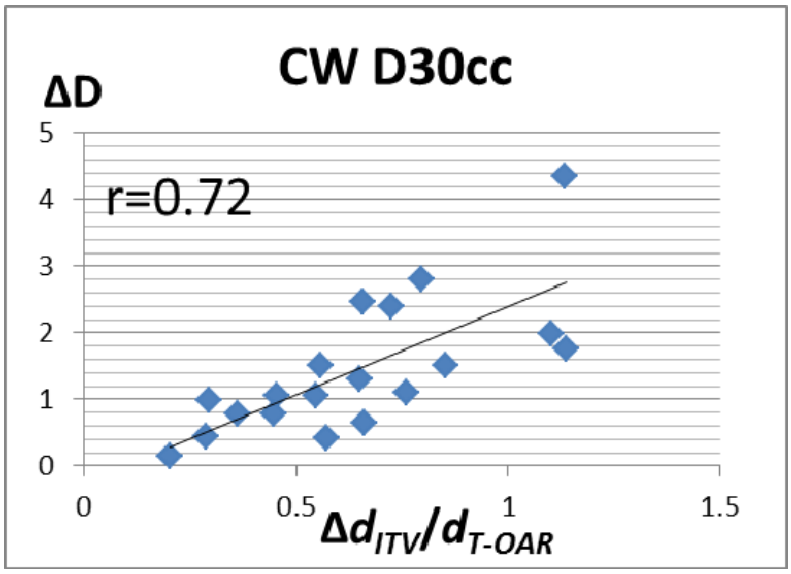

Figure 10: Correlation between $\Delta d_{ITV}/d_{T\text{-}OAR}$ and ΔD30cc of chest wall.

When we look at the chest wall metric of ΔD30cc, stronger correlations between $\Delta d_{ITV}/d_{T\text{-}OAR}$ and ΔD30cc were discovered for sub-grouped peripheral and central tumor patients (r=0.82 and 0.94, respectively) compared to all patients, as shown in Fig. 11-12. It should be noted that the definitions of peripheral and central tumor in our study is different from radiation oncology medical terms. Peripheral tumors in our study are defined as tumors adjacent to the chest wall; central tumors are those away from the chest wall. The stronger correlations indicated that it may be more meaningful in future chest wall studies to perform separate analysis for peripheral and central tumors. In Fig.11, steeper slope is observed for the correlation plot of peripheral tumor, indicating the stronger effect $\Delta d_{ITV}/d_{T\text{-}OAR}$ has on ΔD30cc of chest wall. This is partially due to the fact that $d_{T\text{-}OAR}$ for peripheral tumors (which is essential the radius of ITV) is much smaller than that for central tumors; same ΔITV will lead to greater dose sparing at chest wall for peripheral tumors.

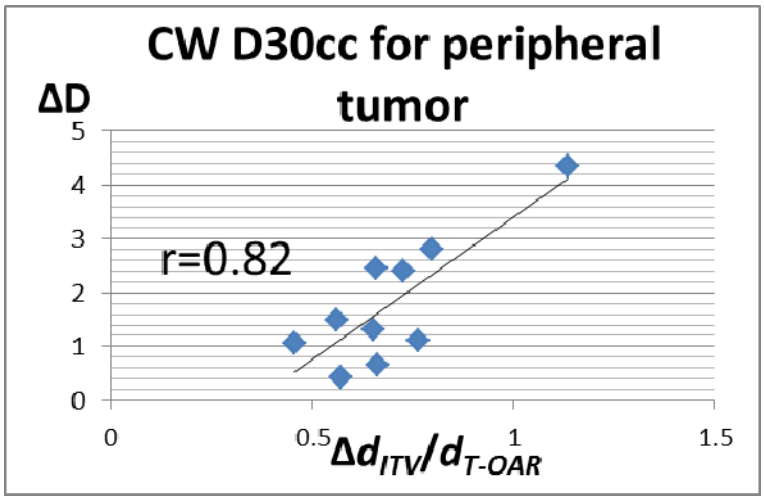

Figure 11: Correlation between $\Delta d_{ITV}/d_{T\text{-}OAR}$ and ΔD30cc of chest wall for peripheral tumors

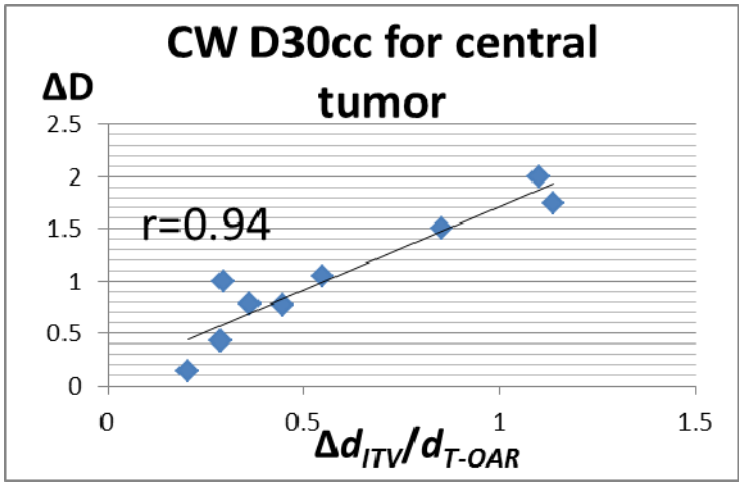

Figure 12: Correlation between $\Delta d_{ITV}/d_{T\text{-}OAR}$ and ΔD30cc of chest wall for central tumors

For spinal cord, no correlation was initially observed between $\Delta d_{ITV}/d_{T\text{-}OAR}$ and its metrics (ΔD1.2cc and ΔD0.35cc). This is largely due to two IMRT patients planned with tight cord constraints (indicated in red in Figs.13-14). Maximum cord sparing was already achieved in the original plan, as shown by Fig.15. In this patient's case, IMRT of

the original CT plan achieved good cord sparing, with the 30% isodose line (light green line) avoiding the cord contour. Adaptive planning thus led to very limited additional dose saving for the cord, as shown by the small or negative values of the red points in Fig. 14-15. If excluding these two data points, good correlations were recovered between $\Delta d_{ITV}/d_{T\text{-}OAR}$ and ΔD1.2cc and ΔD0.35cc of cord (r=0.75 and 0.71, respectively). No such outliners exist for the esophagus or chest wall because for all 5 IMRT cases included in our study, none of them was planned initially with tight esophagus or chest wall constraints.

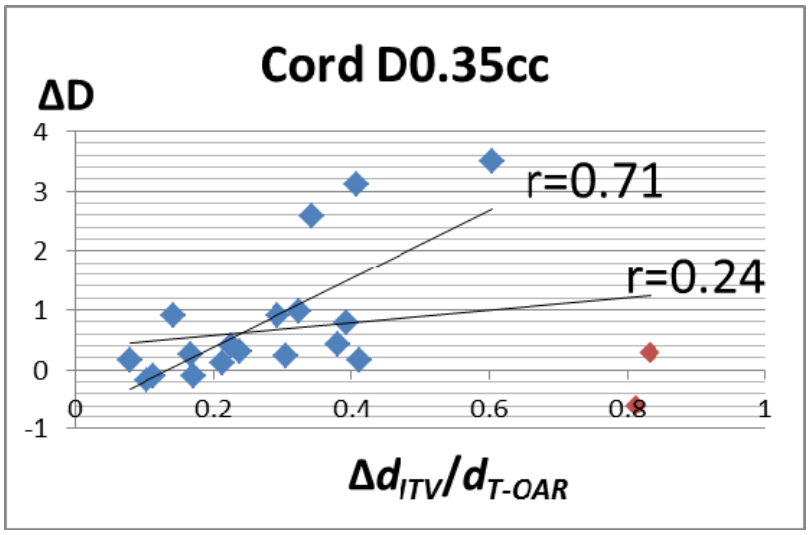

Figure 13: Correlation between $\Delta d_{ITV}/d_{T\text{-}OAR}$ and ΔD0.35cc of cord with (r=0.24) and without (r=0.71) the two IMRT cases with tight cord constraints (red points)

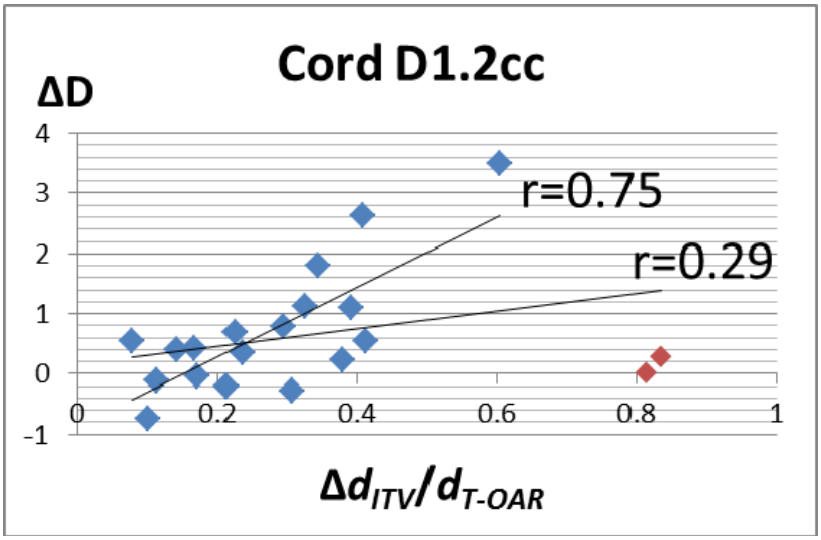

Figure 14: Correlation between $\Delta d_{ITV}/d_{T\text{-}OAR}$ and ΔD1.2cc of cord with (r=0.29) and without (r=0.75) the two IMRT cases with tight cord constraints (red points)

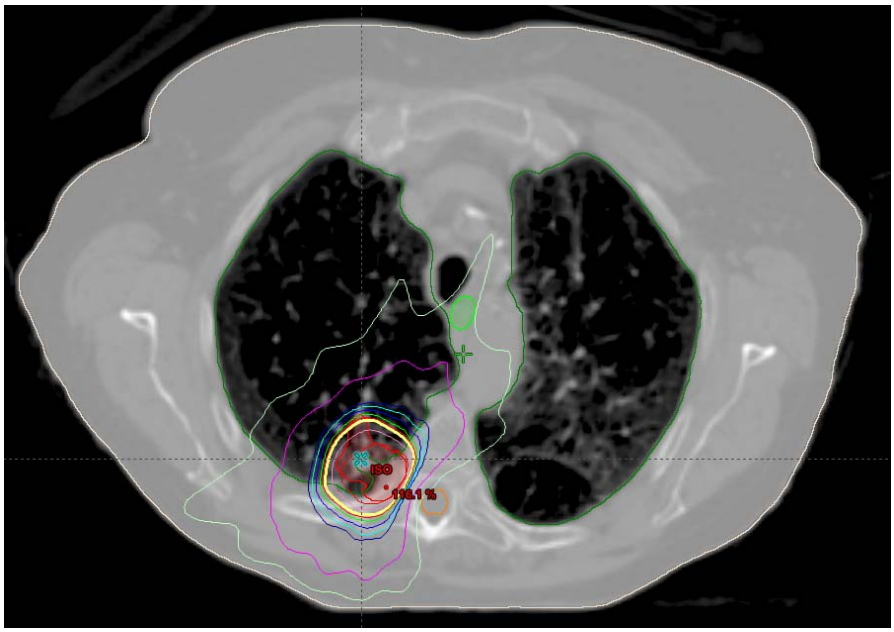

Figure 15: CT plan of one of the two IMRT cases with tight cord constrains. Orange contour represents the cord; thick yellow isodose line is 100%; outermost green isodose line is 30%.

4. Discussion

4.1 Interpretation of Results

In this study we retrospectively investigated the dosimetric effect of adaptive planning on 20 selected lung SBRT patients who presented relatively large target volume changes (percentage ITV change > 15%). We found that compared to non-adaptive planning, adaptive planning significantly reduced radiation dose to OARs (lungs, cord, esophagus, and chest wall) for these studied patients. Given the hypo-fractionated nature of lung SBRT, even small dose reductions to OARs could lead to significant reduction in normal tissue complication probability (NTCP) [13].

The dosimetric advantage calculated in our study is only a conservative estimation, because the actual non-adaptive plan dose may be more than what we calculated. During non-adaptive planning, due to the tumor shrinkage, extra dose was delivered to the normal tissues (mostly lung tissues) surrounding the PTV in later fractions. Our dose accumulation simply assumed the same amount of dose plan for all fractions, therefore underestimating total dose delivered to the OARs. The actual non-adaptive plan may have higher OAR radiation toxicity, and thus larger amount of dose sparing after adaptive planning.

It should be noted that the quantitative results of this study cannot be generalized to all lung SBRT patients. The aim of this study was to quantitatively evaluate potential dosimetric benefits of adaptive planning for lung SBRT patients who

presented relatively larger target volume changes during the treatment. It was not our intention, neither clinically interesting in our opinion, to compare dosimetric performance between adaptive planning and non-adaptive planning for a general population, as we know patients with small target volume changes are less likely to profit from adaptive planning due to anticipated small dosimetric changes.

We used percentage ITV change as a metric for patient selection in this study. For the selected patients, two patient-specific factors, ITV change (or effective tumor diameter change) and tumor-to-OAR distance, were proven to affect the effectiveness of adaptive lung SBRT. It should be noted, however, that neither of these factors can be used as predicting factors for adaptive lung SBRT of a general population, because larger percentage target volume change is a pre-requirement. Although predicting who may profit from adaptive lung SBRT prior to treatment is of extreme clinical interest, it is practically difficult to do so as one cannot foretell whether and how much the target volume will change during the treatment for a particular patient. Nevertheless, patients presented with larger tumor volume changes in the first few fractions are intuitively better candidates for adaptive SBRT. In our study, the patient selection threshold happens to be 15%.

In order to investigate the effect of adaptive lung SBRT on smaller ITV reduction patient, we also carried out adaptive planning on 6 patients with percent ITV reduction smaller than 15%, in addition to the 20 selected patients. Their respective inter-fractional

ITV reductions are: 14.3%, 13.8%, 10.9%, 9.4%, 3.2%, and 0.3%. The same dosimetric analysis was done; and correlation studies were repeated including these 6 patients.

Figures 16-19 are the correlation plots for esophagus, chest wall, and spinal cord with and without the additional 6 patients. For all three OARs, the new r values (in red) are comparable to the old values (in blue). The ratio between effective ITV diameter reduction and tumor-to-OAR distance is still strongly correlated with the dose sparing at all three OARs. These results proved that the exclusion of patients with smaller percent ITV reduction did not affect our results. The same predicting factors were discovered for adaptive lung SBRT.

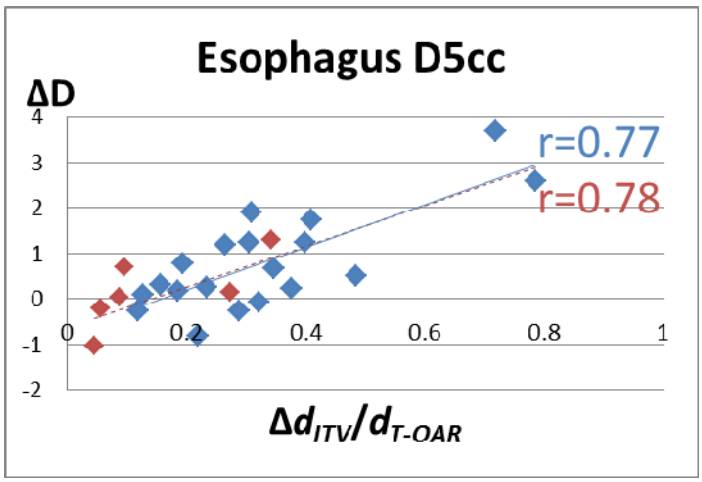

Figure 16: Correlation between $\Delta d_{ITV}/d_{T\text{-}OAR}$ and ΔD5cc of esophagus for 20 selected patients (blue points, blue trend line, blue r value), and 26 patients (all points, red trend line, red r value) with 6 additional small-ITV-change patients in red.

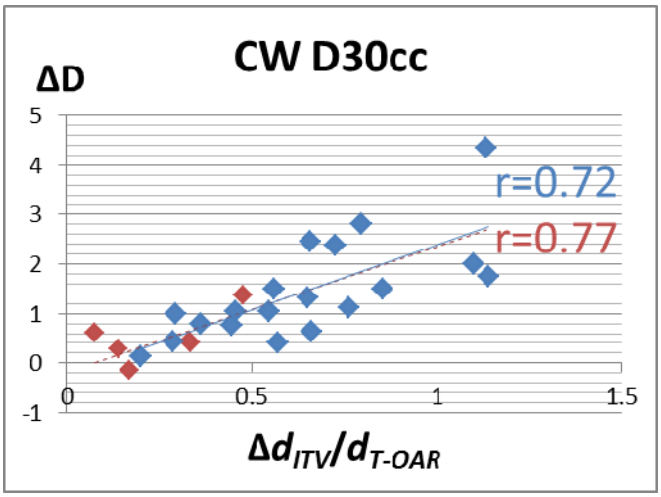

Figure 17: Correlation between $\Delta d_{ITV}/d_{T\text{-}OAR}$ and ΔD30cc of chest wall for 20 selected patients (blue points, blue trend line, blue r value), and 26 patients (all points, red trend line, red r value) with 6 additional small-ITV-change patients in red.

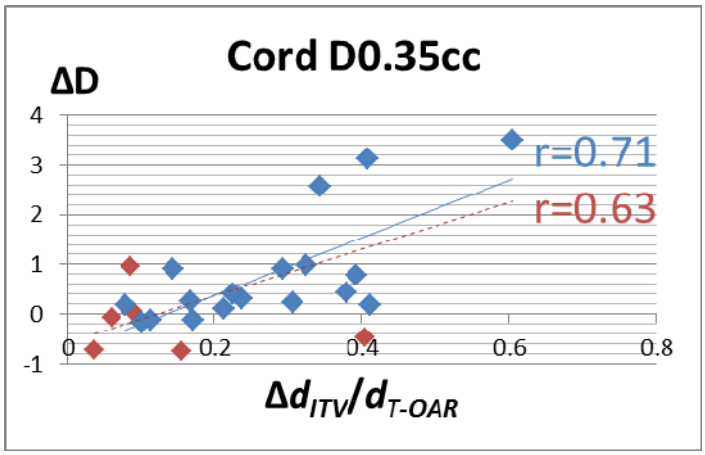

Figure 18: Correlation between $\Delta d_{ITV}/d_{T\text{-}OAR}$ and ΔD0.35cc of spinal cord for 20 selected patients (blue points, blue trend line, blue r value), and 26 patients (all points, red trend line, red r value) with 6 additional small-ITV-change patients in red.

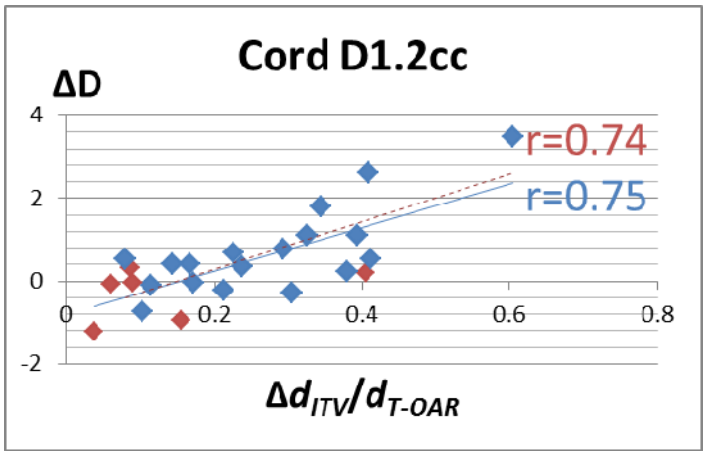

Figure 19: Correlation between $\Delta d_{ITV}/d_{T\text{-}OAR}$ and ΔD1.2cc of spinal cord for 20 selected patients (blue points, blue trend line, blue r value), and 26 patients (all points, red trend line, red r value) with 6 additional small-ITV-change patients in red.

Adaptive strategy can be applied to either shrinking or expanding tumors. In the case of tumor growth, adaptive strategy is able to maintain the new target coverage while sparing OARs. This situation, however, is not the focus of our study because first, it is not very commonly observed in clinic; second, the average percent target volume increase is often much smaller than that of percent target volume decrease. Among the 40 patients of our study shown in Fig. 1, the maximum tumor volume increase is only about 15%.

Despite of a clear threshold for patient selection, large tumor volume reduction and small tumor-to-OAR distance are still useful indicators for adaptive lung SBRT. In our vision, adaptive lung SBRT should be automatic, on-line, and real-time. This is feasible due to the relatively simple geometric relationships between target volume and OARs, as well as relatively simple planning. On-line adaptive lung SBRT can best adapt

the treatment to patient's anatomy and function of the day at each fraction. In addition, on-line adaptive lung SBRT can potentially further reduce safety margins by eliminating the requirement for setup uncertainties.

4.2 Concerns and Limitations

Feasibility of CBCT-based treatment planning has been previously investigated. Yoo *et al*. studied the Hounsfield Unit (HU) value difference between CBCT and CT images for both homogeneous and inhomogeneous Catphan phantoms, as well as various tissue regions of patients. The monitor unit (MU)/cGy differences were found to be within 1% for phantom cases, and the discrepancy between isodose lines were found to be within 2 mm for the patient studies [14]. Yang *et al.* evaluated the dose difference between CT-based planning and CBCT-based planning. It was found that the dose difference between the two was within 2%. However, MU and dose differences can be higher (3%) in the lungs due to respiratory motion. Both studies suggest that CBCT can be employed directly in dose calculation with minimal MU/dose differences [15]. Inter-observer variance in contouring also introduces limited error to CBCT based treatment planning [16]. Nonetheless, current CBCT technique is unable to provide the same image quality as CT. Target volume delineation and dose calculation based on CBCT could therefore contain systematic errors. Impact of CBCT-related uncertainties on our study, however, is expected to be limited since all comparisons were performed on the same imaging modality. Investigation on the comparability between CBCT-based and CT-

based lung SBRT planning is of extreme importance for clinical implementation of adaptive lung SBRT, and is a topic of our future study.

Microscopic disease (MD) associated with the shrinking tumor is a concern in adaptive lung SBRT. The question remains whether the dose reduction in gross tumor volume (GTV) would under-dose the MD around the visible tumor. Since currently there is no imaging technique that is capable of imaging MD beyond the tumor boundary, the extent of MD is typically calculated using special probability models. Guckenberger *et al*. evaluated doses to MD in adaptive radiation therapy for NSCLC lung cancer using a tumor control probability model. Two types of MD movement were studied in the model: synchronous shrinkage of MD and GTV, and stationary MD despite a shrinking GTV [17]. It was shown that dose coverage on MD was not compromised in either situation. Sonke *et al.* suggested that the dose required for MD beyond the visible tumor may be significantly lower than the dose for the GTV [18]. The current study implemented 95% dose coverage on 100% volume of the GTV in adaptive SBRT planning. Over 80% dose coverage was achieved by adaptive plans on the initial GTV volume, indicating a good coverage on MD.

Deformable image registration is an essential component of adaptive treatment planning. Fractional doses associated with different CBCT images cannot be added together, unless they are deformed to the same image first. In addition, since non-adaptive plan dose was calculated based on $CBCT_1$, adaptive plan dose needs to be

based on the same image for accurate comparison. Deformable registration allowed us to deform doses associated with later fraction CBCTs to $CBCT_1$.

The uncertainties and limitations for deformable registration are well recognized, but extremely difficult to measure. This study brought another layer of complexity to the issue, which is how to handle disappearing tumor voxels due to tumor shrinkage. Ideally, deformable registration should match OARs without deforming the tumor. Figure 20 shows an example of deformable registration between $CBCT_4$ and $CBCT_1$ for the case illustrated in Fig. 6-8. It can be seen that deformable registration resulted in good matches in trachea, esophagus, chest wall, and soft tissues, while largely maintained differences in tumor volumes (shown in greyscale color, indicated by yellow arrows). Nevertheless, limited accuracy of deformable registration in regions of disappearing tumor voxels could cause certain level of dosimetric uncertainties in adjacent OARs and the target volumes. Cautions should be taken when interpreting quantitative results of this study.

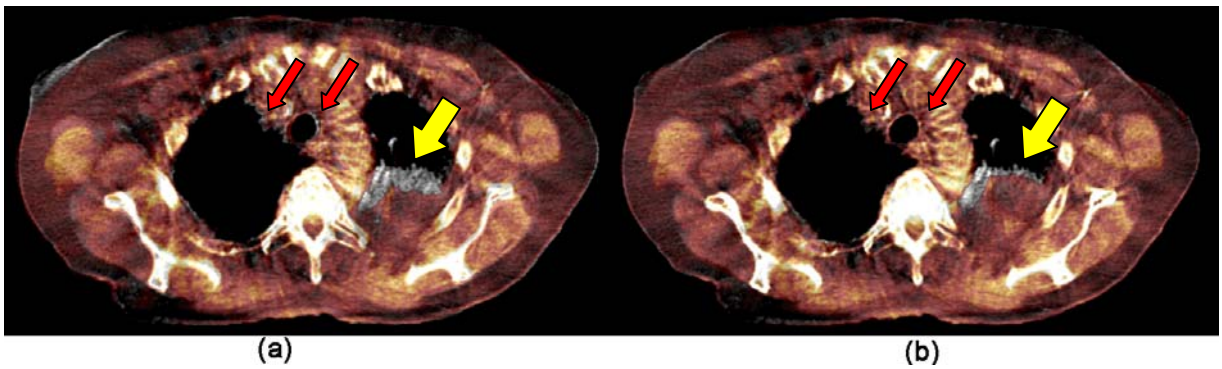

Figure 20: Overlay of CBCT4 and CBCT1 (same case as illustrated in Figs. 5-7 and Table 3) (a) after rigid registration but before deformable image registration; and (b)

after both the rigid and deformable image registration. Red arrows indicate good matches for trachea and soft tissues, while yellow arrows indicate largely maintained differences in tumor volumes (greyscale areas).

5. Conclusions

The purpose of the current study was to assess the effectiveness of adaptive lung SBRT on patients with larger tumor volume changes.

For patients with over 15% tumor volume reduction, adaptive lung SBRT planning significantly reduced dose to adjacent OARs, including lungs, esophagus, spinal cord, and chest wall, while maintaining the same dose coverage to target. Clinical application of adaptive lung SBRT therefore has the potential to further reduce normal tissue toxicity and/or escalate target dose, in order to improve local control and survival rate.

Two patient-specific factors: target volume changes and tumor-to-OAR distances, was found to correlate with the effectiveness of adaptive strategy. These factors are related to patient intrinsic characteristics, therefore can be used in predicting potential candidates for adaptive lung SBRT. However, special attention is required because large percentage tumor reduction is a pre-requirement.

Future studies should work on developing clinical implementation of adaptive lung SBRT that is real-time, on-line, and automatic. Some of the major research directions should include (1) increasing the number of patients for more statistically meaningful results; (2) comparability study of CT versus CBCT-based target delineation and treatment planning; and (3) quantitatively addressing the accuracy of deformable registration in dose accumulation of adaptive plans.

Appendix – List of Abbreviations

3D-CRT – 3-Dimensional Conformal Radiation Therapy

AIP – Average Intensity Projection

ART – Adaptive Radiation Therapy

BED – Biologically Effective Dose

CBCT- Cone-beam Computed Tomography

CI – Conformality Index

DVH – Dose Volume Histogram

EPID – Electronic Portal Imaging Devices

FOV – Field of View

GTV – Gross Tumor Volume

HU – Hounsfield Unit

IMRT – Intensity Modulated Radiation Therapy

ITV – Internal Target Volume

kV – kilo-voltage

MD – Microscopic Disease

MIP – Maximum Intensity Projection

MLC – Multi-Leaf Collimator

MU – Monitor Unit

MV – mega-voltage

NSCLC – Non-small Cell Lung Cancer

NTCP – Normal Tissue Control Probability

OAR – Organ at Risk

P_{ADP} – Adaptive Plan in our study

P_{NON} – Non-adaptive Plan in our study

PTV – Planning Target Volume

RTOG – Radiation Therapy Oncology Group

SBRT – Stereotactic Body Radiation Therapy

SD – Standard Deviation

References

1. Armstrong JG, Minsky BD. Radiation therapy for medically inoperable stage I and II non-small cell lung cancer. *Cancer Treat Rev* 1989; 16(4):247-255

2. Dosoretz DE, Katin MJ, Blitzer PH, *et al.* Medically inoperable lung carcinoma: the role of radiation therapy. *Semin Radiat Oncol* 1996; 6(2):98-104.

3. Fakiris AJ, McGarry RC, Yiannoutsos CT, *et al.* Stereotactic body radiation therapy for early-stage non-small-cell lung carcinoma: four year results of a prospective phase II study. I*nt J Radiat Oncol Biol Phys* 2009; 75: 677-682.

4. Salama J, Kirkpatrick J, Yin F-F. Stereotactic Body Radiotherapy Treatment of Extracranial Metastases. *Nature Reviews Clinical Oncology* 2012 Nov 9(11):654-665.

5. Dunlap N, Cai J, Biedermann GB, *et al.* Chest Wall Volume Receiving More Than 30 Gy Predicts Risk of Severe Pain and/or Rib Fracture After Lung SBRT. *Int J Radiat Oncol Biol Phys* 2010; 76(3): 796-801.

6. Timmerman R, Paulus R, Galvin JM, *et al.* Toxicity analysis of RTOG 0236 using stereotactic body radiation therapy to treat medically inoperable early stage lung cancer patients. *Int J Radiat Oncol Biol Phys* 2007; 69, S86.

7. Stephans K. Stereotactic Body Radiotherapy for Stage I Non-Small Cell Lung Cancer. *Cleveland Clinic Journal of Medicine* 2012; 79: e-S26-e-S31.

8. Takeda A, Kunieda E, Ohashi T, *et al.* Stereotactic Body Radiotherapy (SBRT) for Oligometastatic Lung Tumors from Colorectal Cancer and Other Primary Cancers in Comparison With Primary Lung Cancer. *Radiotherapy and Oncology* 2011 Nov; 101(2):255-9.

9. Bissonnette J, Purdie T, Higgins J, *et al.* Cone-Beam Computed Tomographic Image Guidance for Lung Cancer Radiation Therapy. *Int J Radiat Oncol Biol Phys* 2009; 73(3): 927-934.

10. Altorjai G, Fotina I, Lutgendorf-Caucig C, *et al.* Cone-Beam CT-Based Delineation of Stereotactic Lung Targets: the Influence of Image Modality and Target Size on Interobserver Variability. *Int J Radiat Oncol Biol Phys* 2012; 82(2): e265-e272.

11. Kelly P, Balter P, Rebueno N, *et al.* Stereotactic Body Radiation Therapy for Patients with Lung Cancer Previously Treated with Thoracic Radiation. *Int J Radiat Oncol Biol Phys* 2010; 78(5): 1387-1393.

12. Asai Y, Shioyama Y, Ohga S, *et al.* Radiation Induced Rib Fractures after Hypofractionated Stereotactic Body Radiation Therapy: the Risk Factors and Dose-Volume Relationship. *Int J Radiat Oncol Biol Phys* 2012; 84(3): 768-773.

13. Feng M, Kong FM, Gross M, *et al.* Using Fluorodeoxyglucose Positron Emission Tomography to Assess Tumor Volume During Radiotherapy for Non-Small-Cell Lung Cancer and Its Potential Impact on Adaptive Dose Escalation and Normal Tissue Sparing. *Int J Radiat Oncol Biol Phys* 2009;73(4):1228–1234.

14. Yoo S, Yin FF. Dosimetric Feasibility of Cone-Beam CT-Bease Treatment Planning Compared to CT-Based Treatment Planning. *Int J Radiat Oncol Biol Phys* 2006; 66(5): 1553-1561.

15. Yang Y, Schreibmann E, Li T, *et al.* Evaluation of On-Board kV Cone Beam CT (CBCT)-Based Dose Calculation. Physics in Medicine and Biology, 2007; 52: 685-705.

16. Gabriela A, Rotina I, Lutgendorf-Caucig L, et al. Cone-Beam CT-Based Delineation of Stereotactic Lung Targets: The Influence of Image Modality and Target Size on Inter-observer Variability. *Int J Radiat Oncol Biol Phys* 2012; 82(2): e265-e272.

17. Guckenberger M, Richter A, Wilbert J, *et al.* Adaptive Radiotherpy for Locally Advanced Non-Small-Cell Lung Cancer does not Underdose the Microscopic Disease and has the Potential to Increase Tumor Control. *Int J Radiat Oncol Biol Phys* 2011; 81(4): e275-e282.

18. Sonke JJ, Belderbos J. Adaptive Radiotherapy for Lung Cancer. *Seminars in Radiation Oncology* 2010; 20: 94-106.

19. Vergalasova I, Maurer J, Yin FF. Potential Underestimation of the Internal Target Volume (ITV) from Free Breathing CBCT. *Med Phys* 2011; 38(8): 4689-4700.